

RESEARCH ARTICLE

10.1002/2013JC009650

Special Section:

Western Pacific Ocean
Circulation and Climate

Key Points:

- PDO can influence STC in north hemisphere via subduction-induced density change
- Tropic SSTA appears induced by STC and is swept to subtropic by ocean advection
- SST anomaly in subtropic from STC-induced tropic negatively feedbacks to PDO

Correspondence to:

L. Hong,
hong15264283802@163.com

Citation:

Hong, L., L. Zhang, Z. Chen, and L. Wu (2014), Linkage between the Pacific Decadal Oscillation and the low frequency variability of the Pacific Subtropical Cell, *J. Geophys. Res. Oceans*, 119, 3464–3477, doi:10.1002/2013JC009650.

Received 23 NOV 2013

Accepted 21 MAY 2014

Accepted article online 24 MAY 2014

Published online 5 JUN 2014

Linkage between the Pacific Decadal Oscillation and the low frequency variability of the Pacific Subtropical Cell

Lingya Hong¹, Liping Zhang^{2,3}, Zhaohui Chen¹, and Lixin Wu¹

¹Physical Oceanography Laboratory/Qingdao Collaborative Innovation Center of Marine Science and Technology, Ocean University of China, Qingdao, China, ²Atmospheric and Oceanic Science, Princeton University, Princeton, New Jersey, USA, ³NOAA/Geophysical Fluid Dynamics Laboratory, Princeton, New Jersey, USA

Abstract The decadal variability of Pacific Subtropical Cell (STC) and its linkages with the Pacific Decadal Oscillation (PDO) are investigated in the present study based on a Simple Ocean Data Assimilation (SODA 2.2.4). It is found that, on decadal time scales, the western boundary and interior pycnocline transports are anticorrelated and the variation of the interior component is more significant, which is consistent with previous studies. The decadal variability of STC in the Northern Hemisphere is found to be strongly associated with PDO. Associated with a positive (negative) phase of PDO, the relaxation (acceleration) of the northeast trades slows down (spins up) the STC within a few years through baroclinic adjustment in conjunction with the subduction of the cold (warm) mixed-layer anomalies in the extratropics. The cold (warm) water is then injected into the thermocline and advected further southwestward to the tropics along the isopycnal surfaces, leading to the slowdown (spin-up) of STC due to zonal pressure gradient change at low latitude. Along with the STC weakening (strengthening), a significant warming (cold) anomaly appears in the tropics and it is advected to the midlatitude by the Kuroshio and North Pacific currents, thus feeding back to the atmosphere over the North Pacific. In contrast to the Northern Hemisphere, it is found the STC in the south only passively responds to the PDO. The mechanism found here highlights the role of the STC advection of extratropical anomalies to the tropics and horizontal gyre advection of the tropical anomalies to the extratropics in decadal variability of the STC and PDO.

1. Introduction

The Pacific Subtropical Cell (STC) is a shallow meridional overturning cell, which consists of subduction in the subtropics, equatorward advection of cool subsurface water into the tropics, upwelling at the equator, and poleward advection of warm surface water back to the midlatitudes [McCreary and Lu, 1994; Malanotte-Rizzoli et al., 2000; Schott et al., 2004]. Water masses that are subducted into the thermocline in the eastern subtropics of both hemispheres are swept westward by the North/South Equatorial Currents (NEC/SEC) and reach the equator via the western boundary currents/undercurrents and the interior pathways ultimately. In the equator, the subsurface water from the midlatitude flows into the eastward Equatorial Undercurrent (EUC), subsequently lifts to the surface and eventually comes back to the midlatitude by surface Ekman transports [Huang, 2010].

Observations and ocean reanalysis data indicate that Pacific STC varies on both interannual and decadal time scales [McPhaden and Zhang, 2002, 2004; Schott et al., 2007, 2008; Zhang et al., 2011a]. On interannual time scales, the interior STC convergence is characterized by decreasing during the El Niño events and increasing for the La Niña events as a result of changes in the Sverdrup transport convergence [McPhaden and Zhang, 2002; Schott et al., 2008]. On decadal time scales, McPhaden and Zhang [2002] reported that there is a decadal decline of the STC convergence by about 12 Sv ($1 \text{ Sv} = 1 \times 10^6 \text{ m}^3 \text{ s}^{-1}$) from the mid-1950s to the mid-1990s and this decrease was further confirmed by the warming of the equatorial upwelling waters. Subsequently, McPhaden and Zhang [2004] found a substantial increase of STC convergence accompanied by cooling of equatorial upwelling waters from the mid-1990s to 1998–2003. Using German partner for Estimating the Circulation and Climate of the Ocean (GECCO) assimilation data, Schott et al. [2007] argued that the interior Pacific STC convergence exhibits less significant decadal weakening from the 1960s to the 1990s than hydrographic estimations in previous studies [McPhaden and Zhang, 2002]. The reduction of interior STC convergence from the 1960s to the 1990s and then a rebound in the early 2000s is

also verified by SODA 2.0.2/3 [Schott *et al.*, 2008] and it is in agreement with the STC tendencies indicated by McPhaden and Zhang [2002, 2004].

The mechanism of the Pacific decadal STC variability is not clear so far. McPhaden and Zhang [2002, 2004] suggested that the decadal climate shift over the Pacific basin may contribute to the STC decadal variations. The Pacific Decadal Oscillation (PDO), which has a horseshoe-like spatial SST pattern, is the most significant decadal variability in the Pacific Ocean [e.g., Latif and Barnett, 1994; Mantua *et al.*, 1997]. It is found that the 1976/1977 regime shift of PDO from its negative phase to positive phase is accompanied by a slowdown of the STC [McPhaden and Zhang, 2002]. Also, the rebound of STC in the late 1990s coincides with another PDO regime shift from its positive phase to negative phase [McPhaden and Zhang, 2004]. Moreover, Kleeman *et al.* [1999] suggested that the PDO can affect the equatorial zone through an oceanic teleconnection that involves transport variations of the North Pacific STC. On the other hand, the STC plays a significant role in decadal variability of the Pacific climate. Gu and Philander [1997] argued that such a subtropic-tropic link is, in principle, responsible for interdecadal climate fluctuations over the Pacific Ocean, implying the relationship between STC and PDO. However, the linkages between them still remains poorly understood due to lack of long-term observations, which imposes an obstacle to detect changes of the Pacific decadal shift. In this study, we attempt to investigate the STC decadal variability and its linkages with the PDO based on a newly developed ocean data assimilation product spanning from 1871 to 2008.

The paper is organized as follows: section 2 introduces the data sets and methods used in this study. The mean and decadal variability of STC are described in section 3. Sections 4 and 5 present the linkages between the PDO and STC in the North and South Pacific, respectively. The paper is concluded with a summary in section 6.

2. Data Sets and Methods

The Simple Ocean Data Assimilation (SODA, version 2.2.4) [Giese and Ray, 2011] is adopted in this study. For the ocean model, the relevant configurations and the assimilation algorithm, readers can refer to the detailed report on the SODA product [Carton and Giese, 2008]. The variables in SODA are interpolated onto a uniform $0.5^\circ \times 0.5^\circ$ grid, with 40 levels in the vertical direction and monthly average in time. The model's surface boundary conditions are taken from a new atmospheric data set designated as the Twentieth Century Reanalysis version 2 (20CRv2), which contains the synoptic-observation-based estimate of global tropospheric variability spanning 1871–2008 at 6 hourly temporal and 2° spatial resolutions [Compo *et al.*, 2011].

It is conventional that meridional transports near 10°N and 10°S are commonly used to characterize the strength of STC. These latitudes are equatorward of the NEC/SEC bifurcation that separate the tropical and subtropical gyres [e.g., Qu and Lindstrom, 2002; Chen and Wu, 2011]. In addition, 10°N is located at the maximum potential vorticity ridge, which is largely associated with the Ekman pumping in the intertropical convergence zone (ITCZ) region.

Figure 1 exhibits the mean potential vorticity on the 25.0 kg/m^3 potential density surface. Here the potential vorticity (PV) is calculated based on $f (\partial\rho/\partial z)/\rho$, where $\partial\rho/\partial z$ is the density tendency in vertical direction [McPhaden and Zhang, 2002]. It is shown that the maximum PV primarily exists in the northeastern Pacific Ocean and it extends westward along the 9°N – 10°N band, forming a PV ridge. As a check point, the PV ridge

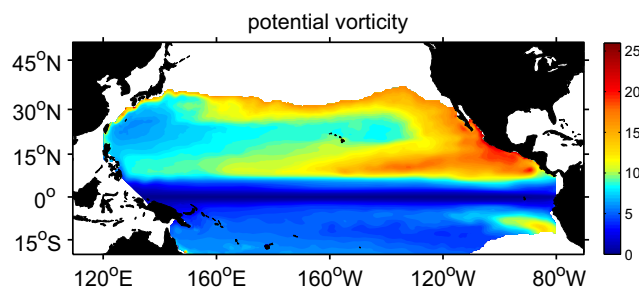


Figure 1. Absolute values of long-term mean (1871–2008) potential vorticity on the 25.0 kg m^{-3} potential density surface. Unit is $10^{-10} \text{ m}^{-1} \text{ s}^{-1}$.

hinders the water from the higher latitudes to the tropics [Johnson and McPhaden, 1999; Lu and McCreary, 1995] and accumulates in turn a large amount of interior water there. Therefore, the strength of Pacific STC can be well represented by the transport across 10°N . To keep symmetry, we choose the meridional transport at 10°S to depict the Southern Hemispheric STC.

Note that water masses subducted in the mid-Pacific flow on isopycnal

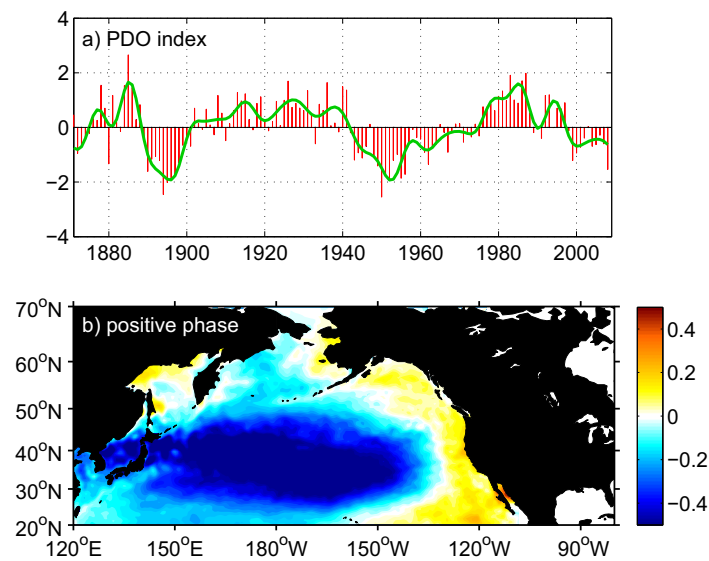


Figure 2. Empirical Orthogonal Function (EOF) decomposition of the annual mean SST anomaly over the North Pacific Ocean (north of 20°N). (a) The first principle time series (red bar), and the green line denotes 7 years low-pass filter. (b) The first EOF spatial pattern. Unit is °C. The first EOF mode accounts for 26% of the total covariance.

leading principle component of the Pacific annual mean SST variability north of 20°N [Mantua et al., 1997], as shown in Figure 2a. It is demonstrated that the PDO primarily oscillates on decadal time scales and its spatial pattern is characterized by a horseshoe-like structure with cooling (warming) in the western and central midlatitude and surrounded by warming (cooling) in the eastern Pacific during the positive (negative) phase (Figure 2b). We will discuss the relationship between STC and PDO in more detail in sections 4 and 5.

3. Mean and Decadal Variability of STC

As shown in Figure 3, same isopycnals are selected following Mcphaden and Zhang [2002, 2004] to mark the top and bottom of the STC layer. It should be noted that we consider the mixed-layer depth (0.125 kg m⁻³ criterion) as the upper boundary when it is denser than

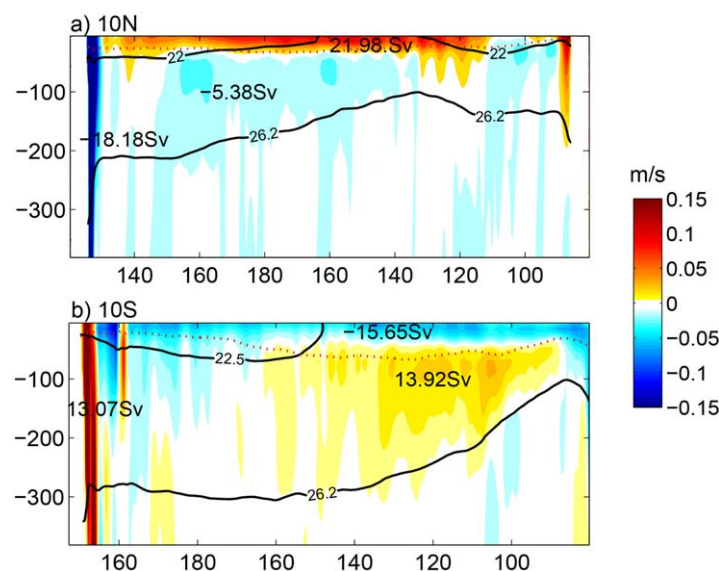


Figure 3. Mean meridional velocity at (a) 10°N and (b) 10°S from SODA 2.2.4 with isopycnals (in kg m⁻³). Also marked are the bottom of the mixed layer (red) and transports (in Sv) of the mixed layer and STC layer (separately for interior and western boundary). The x axis denotes the longitude and the y axis denotes the depth.

surface and they cannot cross PV contours. Since the maximum PV primarily originates in the north-eastern Pacific Ocean (Figure 1), there are two pathways for them to reach the tropical ocean and eventually into EUC: the western boundary currents and the interior passageway. During the PDO events, temperature and salinity anomalies in the mid-Pacific injected into the pycnocline are swept along the PV contours and can reach 10°N, modulating the zonal pressure gradient over there to influence the STC strength. The phase transition in PDO is also associated with the changes in trade wind and the related wind stress curl anomaly along 10°N/S, which affects the STC transport directly.

The PDO index is defined as the leading principle component of the Pacific annual mean SST variability north of 20°N [Mantua et al., 1997], as shown in Figure 2a. It is demonstrated that the PDO primarily oscillates on decadal time scales and its spatial pattern is characterized by a horseshoe-like structure with cooling (warming) in the western and central midlatitude and surrounded by warming (cooling) in the eastern Pacific during the positive (negative) phase (Figure 2b). We will discuss the relationship between STC and PDO in more detail in sections 4 and 5.

the top STC isopycnal (22.0 kg m⁻³ at 10°N and 22.5 kg m⁻³ at 10°S, respectively). The bottom of the STC layer is marked by the 26.2 kg m⁻³ isopycnal in both hemispheres.

The long-term mean equatorward STC transports and poleward Ekman transports during 1871–2008 are shown in Figure 3. In the Northern Hemisphere, the total equatorward STC transport (23.56 Sv) is primarily composed of western boundary current (WBC) with a magnitude about 18.18 Sv, while the equatorward interior transport is only 5.38 Sv (Figure 3a). The total equatorward transports are mostly compensated

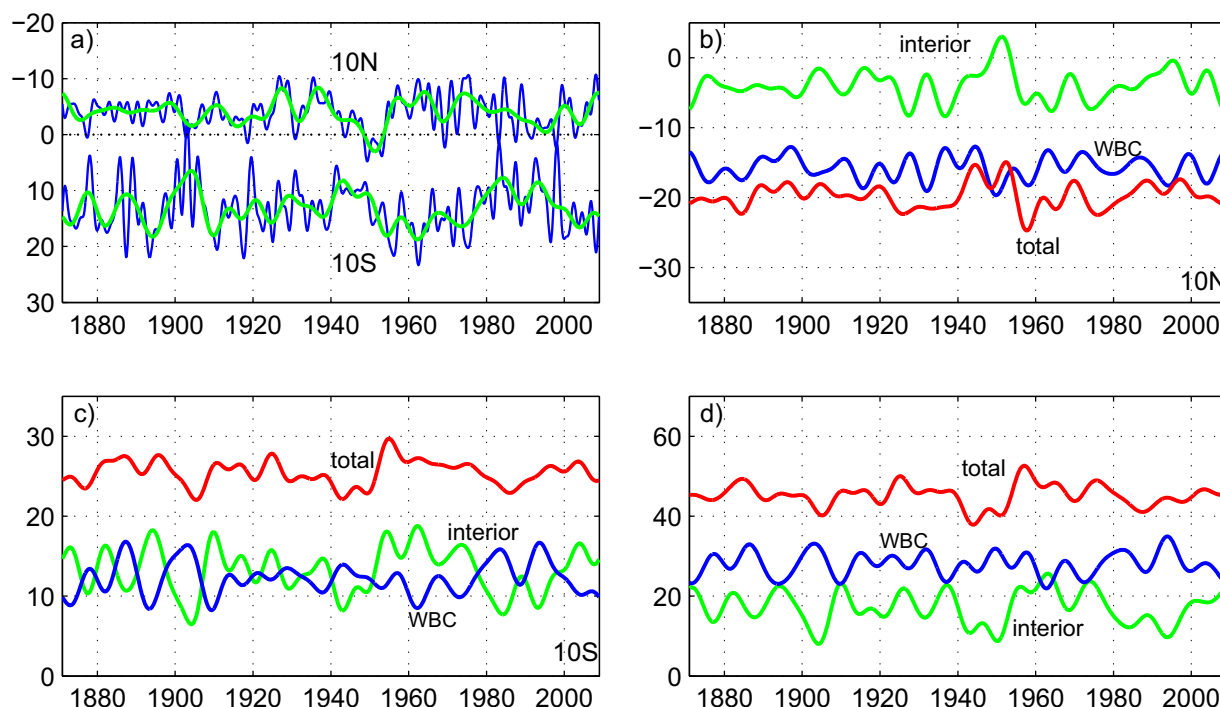


Figure 4. Time series of (a) annually (blue) and 7 years low-pass filtered (green) STC transports for interior that is integrated in the $22.0\text{--}26.2\text{ kg m}^{-3}$ density range from 145°E to 83°W along 10°N and from 160°E to 80°W at 10°S , (b) low-pass (7 years Hanning) filtered interior (green), WBC (blue) and coast-to-coast (red) STC transports at 10°N from SODA, (c) as Figure 4b but for 10°S , and (d) SODA transports for WBC (blue), interior (green) and total (red) STC convergence for $10^{\circ}\text{N}/10^{\circ}\text{S}$ sections. Unit is Sv.

by the poleward mixed-layer transport of 21.98 Sv (Figure 3a). In contrast, the WBC transport and interior transport in the Southern Hemisphere are comparable (13.07 Sv versus 13.92 Sv) and the total transport is partially balanced by the poleward mixed-layer transport (15.65 Sv; Figure 3b). Further calculation reveals that the total STC convergence from both hemispheres reaches 50.55 Sv, whereas the total poleward divergence in the mixed layer is 37.63 Sv. This generates an imbalance of 12.92 Sv within the STC density range and it is eventually exported to the Indian Ocean by the Indonesian Throughflow (figure not shown).

Next, the STC decadal variability is examined. Figure 4a shows the time series of interior STC transports across $10^{\circ}\text{N}/10^{\circ}\text{S}$. On interannual time scales, the transports from respective hemisphere almost fluctuate synchronously with each other with the correlation over 0.4, which is consistent with previous studies [e.g., Schott *et al.*, 2008; Zhang and McPhaden, 2006]. On decadal time scales, the synchrony of interior transports from two hemispheres enhances (correlation $r = 0.51$). The decadal WBC anomalies, as shown in Figures 4b and 4c, reveal the reversed phase with the interior STC variations, leading to the reduced decadal amplitude of the total STC transport in both hemispheres. However, the decadal fluctuations of interior STC transport is not overwhelmed by that of WBC component, so the total STC decadal variation mainly follows the phase of interior STC transport (Figures 4b and 4c) [e.g., Lee and Fukumori, 2003]. It is further found that the decadal variation of total STC transport convergence (Figure 4d) is largely associated with that in the Southern Hemisphere (Figure 4c), whereas the Northern Hemispheric transport plays a minor role in its amplitude (Figure 4b).

4. Linkages Between PDO and STC in the North Pacific

The power spectrum analyses in Figure 5 indicate that both the PDO and STC have strong decadal fluctuations, with a broad peak around 30–50 years. To investigate their linkages in the Northern Hemisphere, a lead-lag correlation is employed between the PDO index and the coast-to-coast STC transport index at 10°N (Figure 6a). It is found that there is a significant negative (positive) correlation of -0.33 (0.50) when the PDO leads (lags) the STC by 10 (2) years and all correlation coefficients exceed the 90% statistic confidence level. When the PDO leads, its positive phase induces a slowdown of the Northern Hemispheric STC

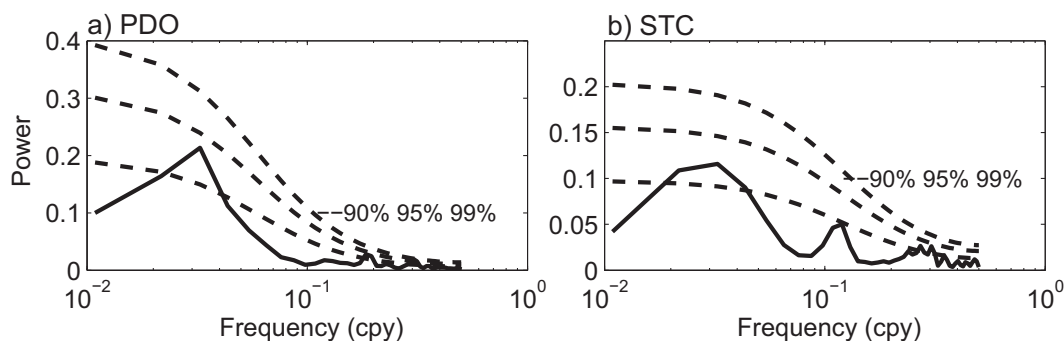


Figure 5. Power spectrum of (a) PDO index and (b) coast-to-coast STC time series at 10°N.

due to the slow adjustment of ocean circulation. Years later, the weakened STC tends to warm the surface water in the tropics and subtropics, followed by the negative phase of the PDO. Its negative phase is in favor of generating a strengthened STC that will further feedback to the PDO years later. The opposite is also true and this periodic feedback oscillates on decadal time scales. The key elements in this oscillation involve the slow adjustment of ocean circulation and related midlatitude ocean/atmosphere responses to STC-induced tropical SST change, which provide possible feedbacks to the entire system.

To further investigate their dynamical relationship, we regress the SST and surface wind stress onto the total STC index with certain years of lead/lag (Figure 7). Consistent with the lead-lag correlation, Figures 7a–7d indicate that the strengthening (weakening) of the STC is largely associated with the negative (positive) phase of the PDO. Before the STC strengthens (weakens), the Pacific Ocean is occupied by a horseshoe-like SST pattern with warming (cooling) in the western and central midlatitude and surrounded by a cooling (warming) anomaly in the east. Associated with the warming (cooling) SST, the surface wind presents anti-cyclone (cyclone) over the North Pacific and the upper ocean heat content displays a positive (negative) anomaly in the midlatitude as a result of the negative (positive) wind stress curl (Figures 8a–8d). The above mentioned SST, heat content, and surface wind anomalies are in good agreement with the negative

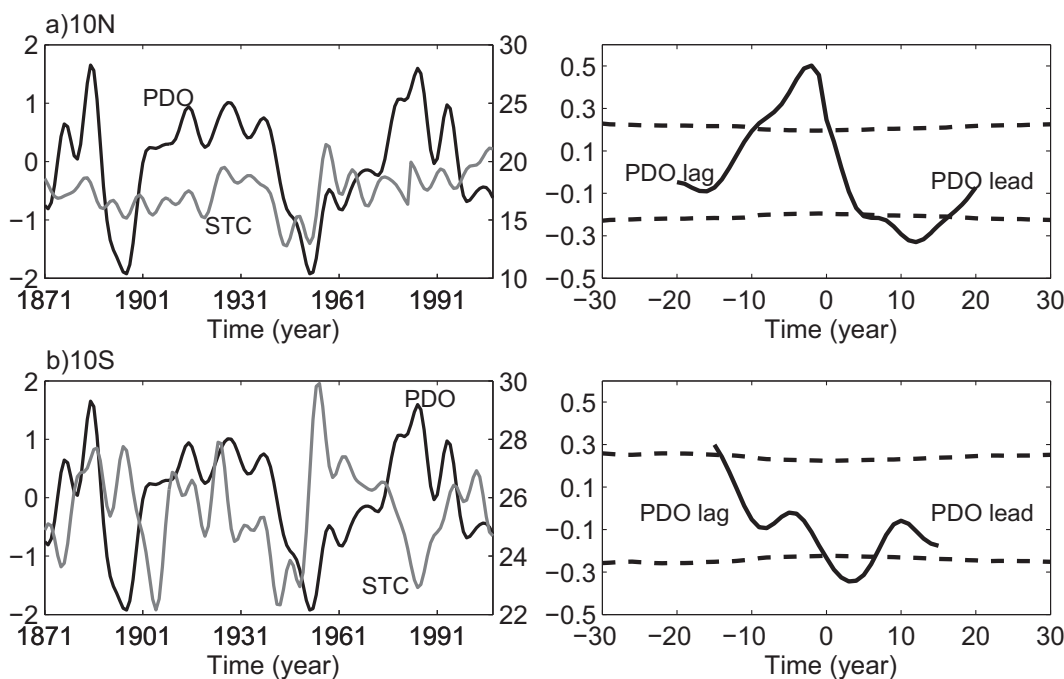


Figure 6. The (left) time series and (right) lead-lag correlation of the PDO index and the decadal STC coast-to-coast transport at (a) 10°N and (b) 10°S, respectively. For the lead-lag correlation, the x axis denotes the years for leads and lags, and the y axis denotes the correlation coefficient. The dash lines denote the statistic 90% confidence level of the t test.

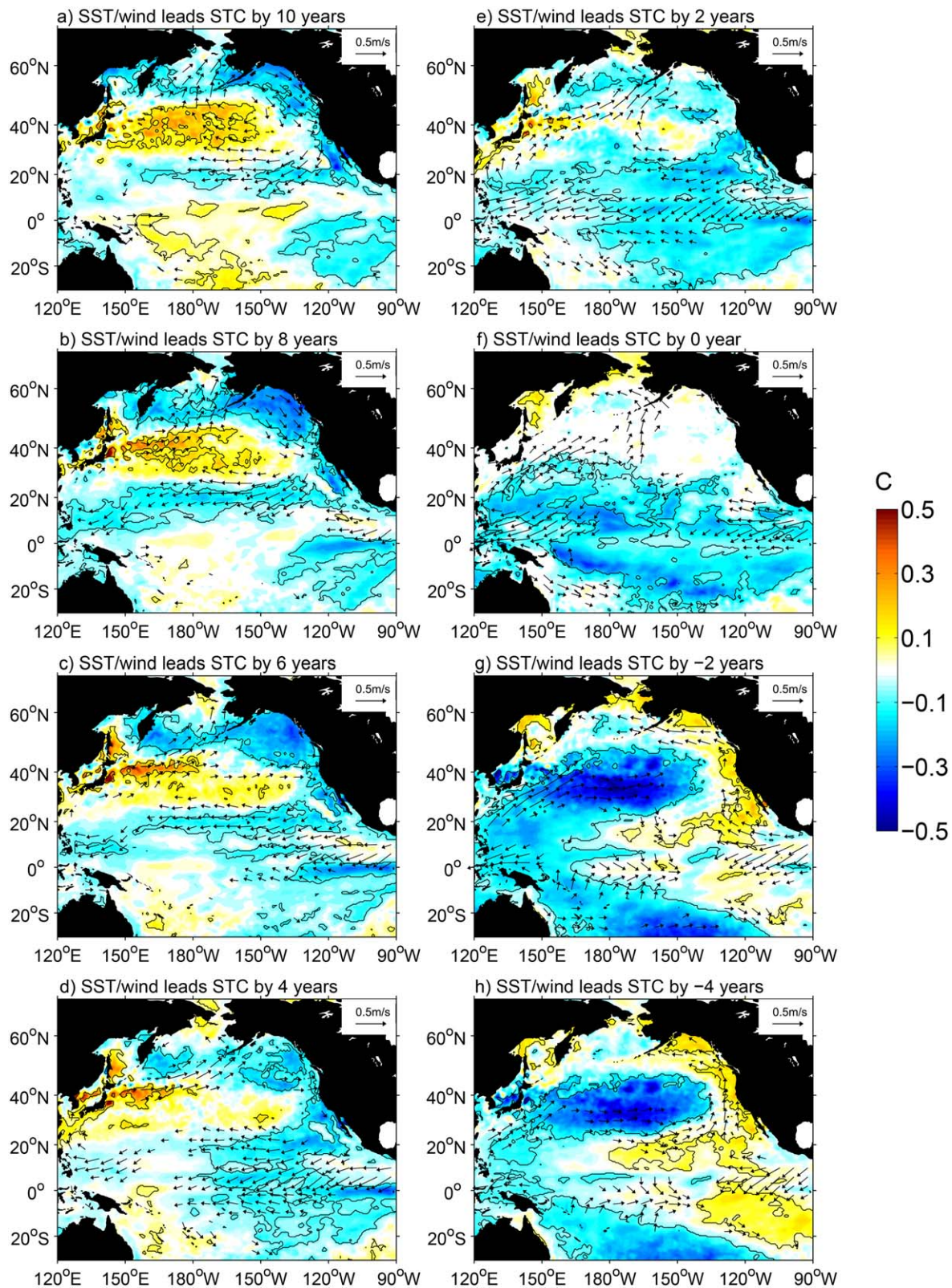


Figure 7. Regression of annual mean SST (shading) and surface wind (vectors) against the STC transport at 10°N. Shown are leaded regressions at (a) 10 years, (b) 8 years, (c) 6 years, (d) 4 years, (e) 2 years, (f) 0 year, (g) -2 years, and (h) -4 years. The contours imposed on the SST shading denote the 90% statistical significance level and only wind regressions exceeding 90% statistical significance are plotted. Units for SST and surface wind are °C and m/s, respectively.

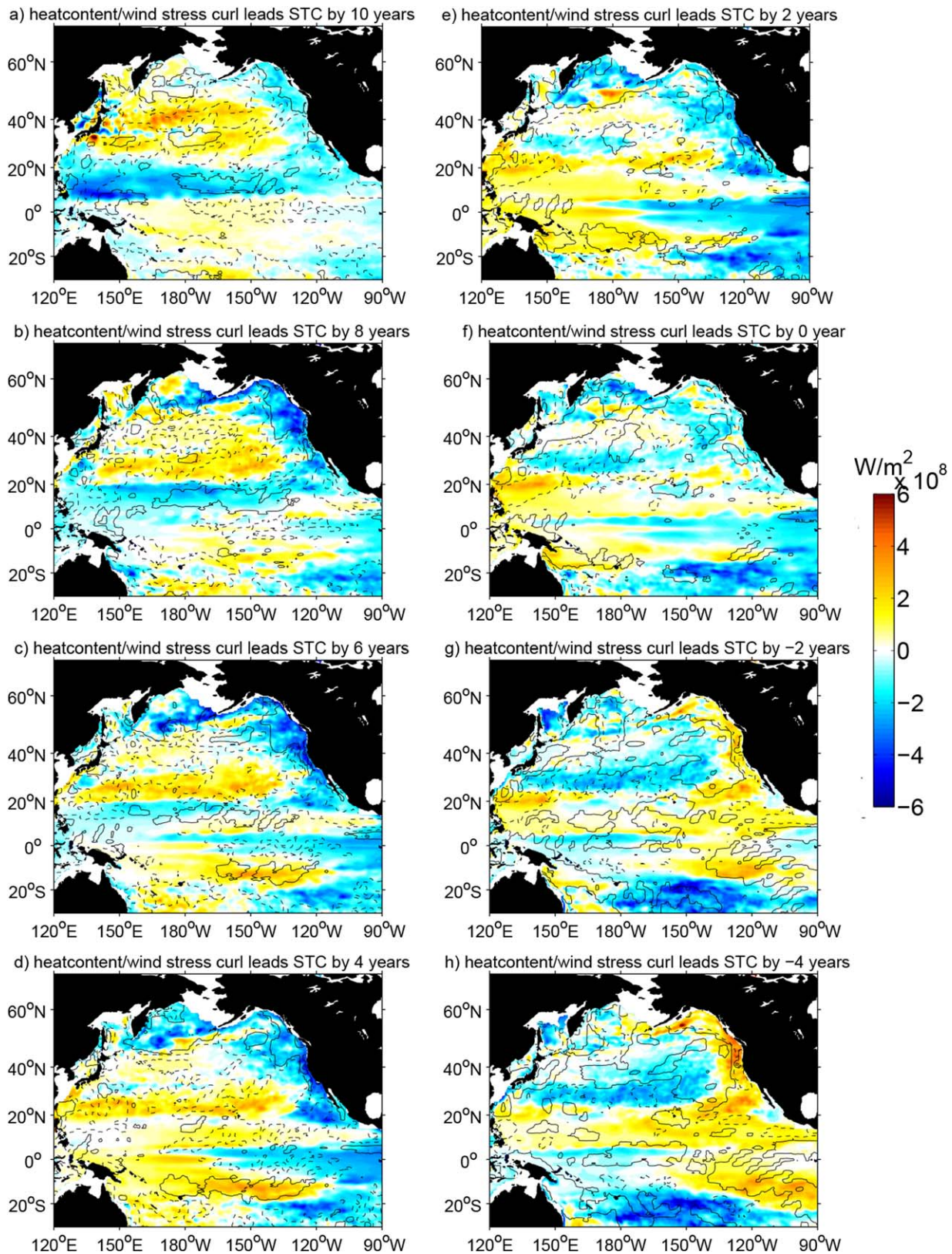


Figure 8. Same as Figure 7 but for the heat content above 400 m (shading, W/m²) and wind stress curl (contours, 10⁻⁹ N/m³) regressions. The solid (dash) contours are 1 (-), 5 (-5), and 10 (-10).

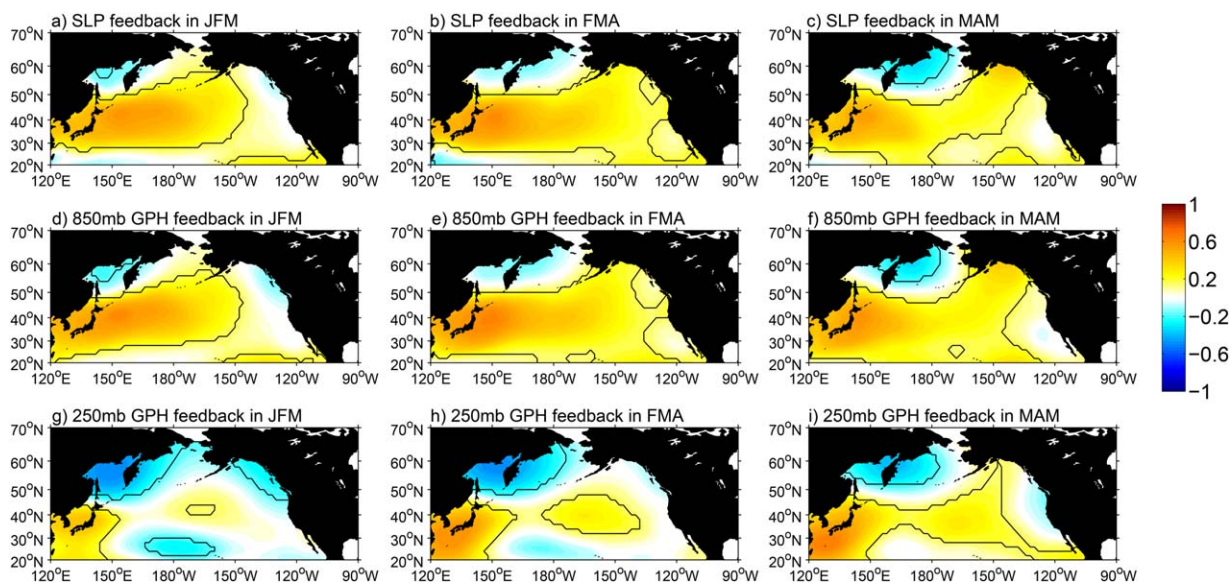


Figure 9. Lagged correlation between the winter SSTAs in the western North Pacific region (DJF, 150°E–180°W, 35°N–45°N) and the sea level pressure in (a) JFM, (b) FMA, and (c) MAM. (d–f and g–i) The same with Figures 9a–9c but for 850 and 250 mb geopotential height, respectively. The contours imposed on the shading denote the 90% statistical significance level.

(positive) phase of the PDO. Accordingly, the anticyclonic (cyclonic) wind strengthens (weakens) trade wind and produces negative (positive) wind stress curl in the subtropics, which favors an increase (a decrease) of the STC. Different from the rapid atmospheric adjustment, the ocean has a large inertia and the response of the STC, particularly the WBC component, to the surface wind, exhibits a delay of several years.

As the STC accelerates (decelerates), more (less) cold water from the subtropics enters the tropics and upwells in the eastern equatorial Pacific, leading to the cooling (warming) SST as well as negative (positive) heat content (Figures 7c–7e and 8c–8e). The positive ocean-atmosphere feedbacks in the tropics [Bjerknes, 1964] amplify this perturbation and cause a significant surface cooling (warming) in the entire tropical region (Figures 7e and 7f). The tropical SST anomalies then gradually spread to the midlatitude by WBC (Figures 7f–7h) and further downstream by the mean zonal current. The western and central midlatitude are finally featured by a cool (warm) anomaly, which favors triggering a low (high)-pressure response in atmospheric circulation (Figures 7g and 7h). This anomalous wind can exert its impact on the ocean, generating a horseshoe-like SST anomaly due to heat flux and horizontal advectations. Therefore, local air-sea coupling in the midlatitude plays a positive feedback role to amplify the initial SST anomaly and eventually reverses the original phase of the PDO (Figures 7g, 7h, 8g, and 8h).

Here the positive air-sea feedback in the midlatitude is consistent with previous studies, in which they investigated the atmospheric response to the midlatitude SST anomaly using atmospheric general circulation models (AGCMs) or atmosphere and ocean coupled models (CGCM) [Palmer and Zhaobo, 1985; Pitcher et al., 1988; Kushnir and Lau, 1992; Peng et al., 1995, 1997; Kushnir and Held, 1996; Latif and Barnett, 1994, 1996; Kushnir et al., 2002; Liu and Wu, 2004; Zhang et al., 2011b, 2011c]. Most of models exhibit a barotropic high (low)-pressure response to a warm (cold) SST anomaly in the midlatitude because of the strong eddy activities and atmospheric internal variability there. At the beginning, the atmospheric response to warm SST is represented by a baroclinic structure, with a low pressure in the low level and a high pressure in the high level. Then, the nonlinear feedback of atmospheric transient eddies can transfer the high level response down to low level, inducing a consistent response in both high and low levels, thus exhibiting a barotropic high response. The lagged correlation is calculated between SSTAs in the western North Pacific and atmospheric variability over the North Pacific (Figure 9). Here we choose the SSTA in the winter time (DJF) when the ocean has the strongest feedback on the atmosphere. We also make the SSTA lead atmospheric variable by 1, 2, and 3 months. Due to atmosphere short persistence, SSTA leading mainly reflects ocean feedback to the atmosphere [e.g., Frankignoul and Sennéchal, 2007]. Figure 9 shows that the atmospheric response to warm (cold) SST anomaly in the western North Pacific is largely barotropic and characterized by a warm ridge (cold trough), which is consistent with previous studies [e.g., Gan and Wu, 2012]. On

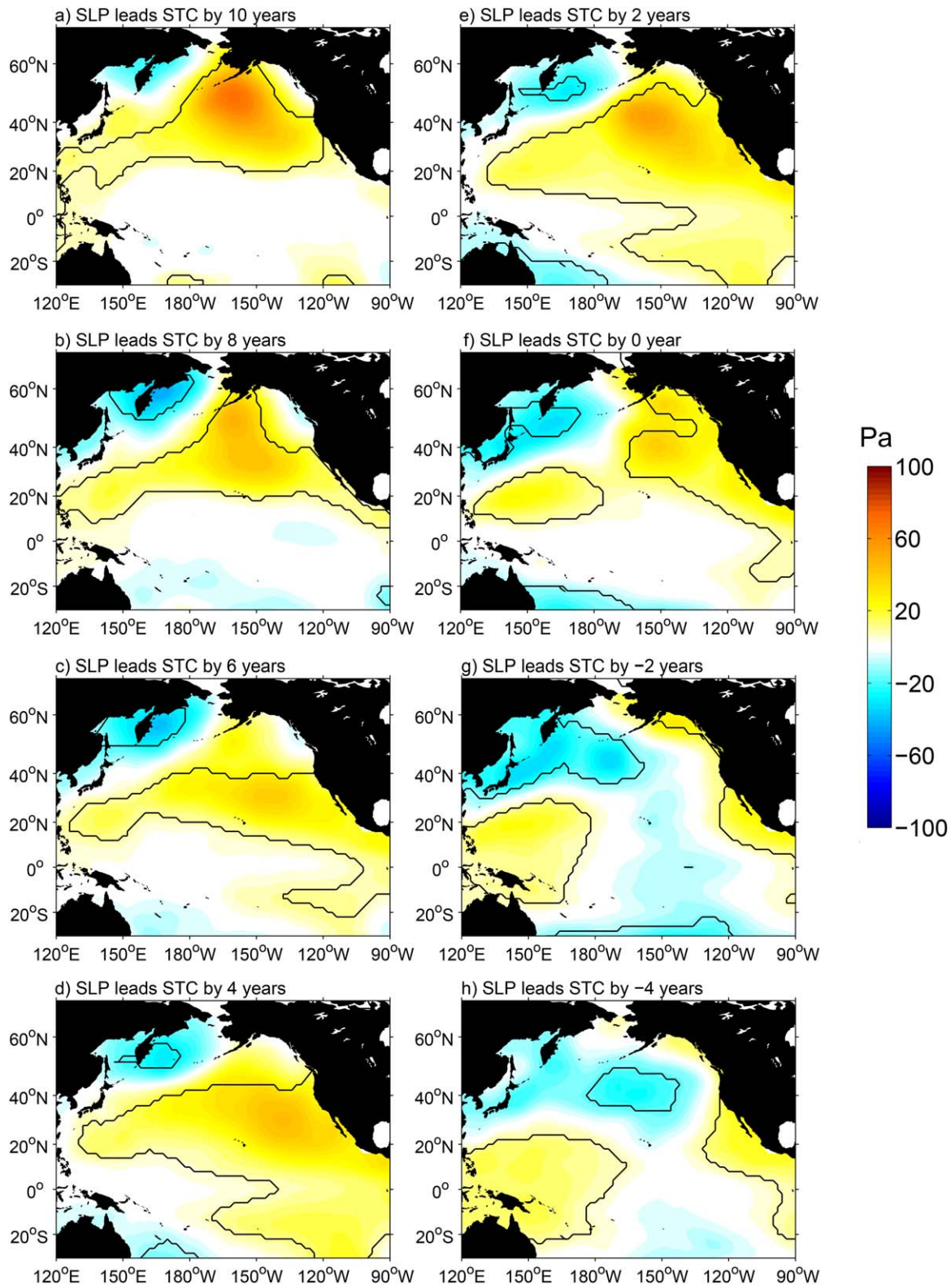


Figure 10. Regression of annual mean surface level pressure (SLP) against the STC transport at 10°N. Shown are the leaded regressions at (a) 10 years, (b) 8 years, (c) 6 years, (d) 4 years, (e) 2 years, (f) 0 year, (g) -2 years, and (h) -4 years. Unit is Pa and the contours imposed on the shading denote the 90% statistical significance level.

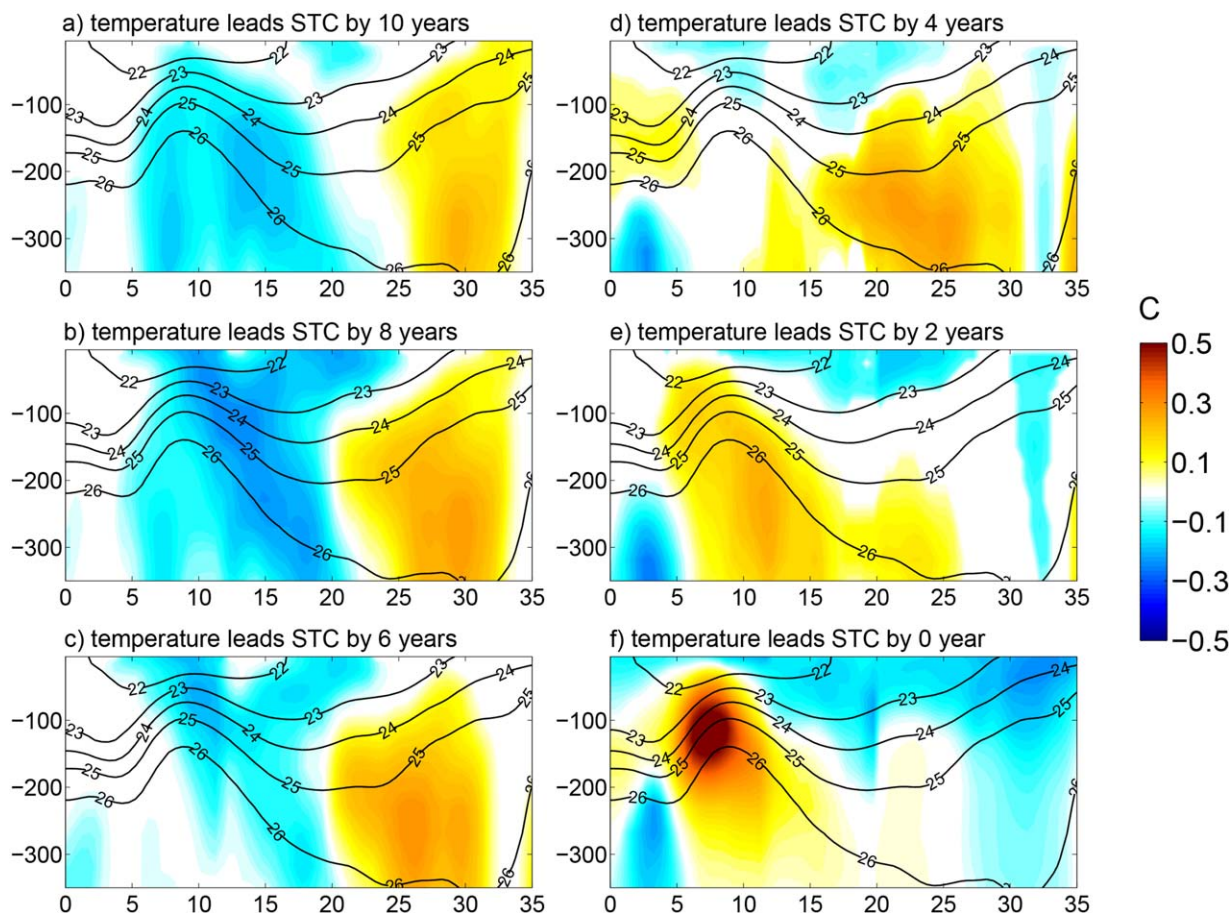


Figure 11. Regression of the zonal averaged (170°E–150°W) temperature profile against the decadal STC transport at 10°N with the climatological potential density (in kg m^{-3}). Shown are led regressions at (a) 10 years, (b) 8 years, (c) 6 years, (d) 4 years, (e) 2 years, and (f) 0 year. The x axis denotes the degree of northern latitude. Unit is $^{\circ}\text{C}$.

the other hand, the high pressure (anticyclonic wind) over the North Pacific Ocean reduces the westerly in the midlatitude, leading to a decreased latent heat loss and an increased northward Ekman transport, both of which can amplify the initial warm anomaly in the midlatitude. The negative wind stress curl associated with the anticyclonic wind favors an accelerating and northward shift of subtropical gyre, producing a warm SST anomaly in the Kuroshio-Oyashio-Extension region. The opposite is also true. Due to this positive air-sea feedback, the midlatitude SST anomaly becomes stronger and stronger (Figure 10).

In the next part, we will demonstrate why there exists a significant negative correlation as the PDO leads the STC (10°N) at interannual to decadal time scales. The PDO can modulate STC through both wind and

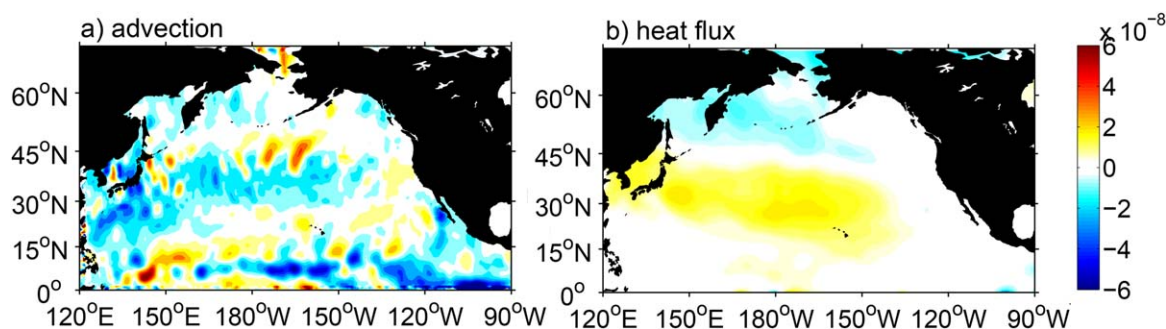


Figure 12. Regression of heat budget terms against the decadal STC transport at 10°N (STC leads the heat budget terms by 2 years). (a) Horizontal temperature advection and (b) surface heat flux. Unit is $^{\circ}\text{C/s}$ and the surface heat flux is downward positive.

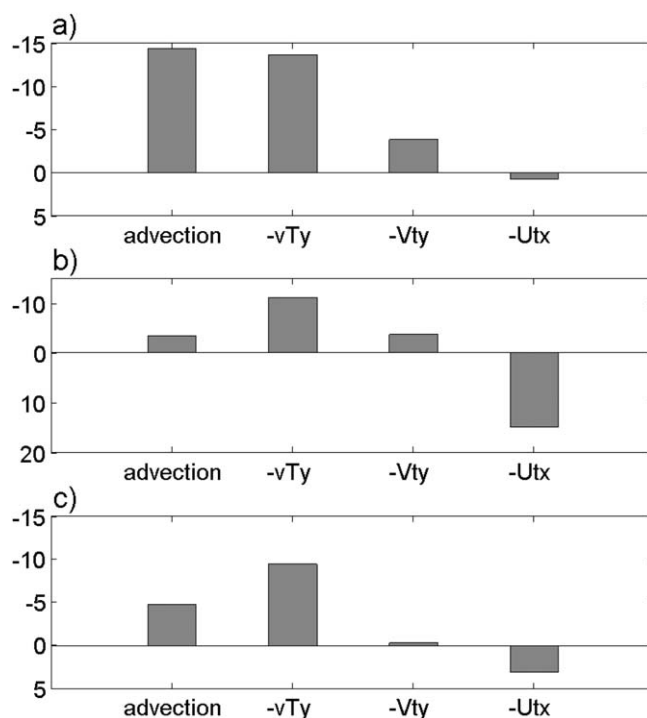


Figure 13. The area averaged heat budget analysis associated with the Northern Hemispheric STC leading 2 years in the (a) KE coastal region (124°E–140°E, 20°N–36°N), (b) KE crest region (140°E–165°E, 30°N–40°N), and (c) KOE region (165°E–180°E, 30°N–40°N). Unit is 10^{-9}C/s .

buoyancy forcing, which can force both first and second baroclinic mode adjustment [e.g., Liu, 1999]. The surface wind anomalies in lower latitudes associated with the PDO can modulate the STC at interannual time scales through baroclinic Rossby wave adjustment, while the subduction of extratropical thermocline anomalies associated with the PDO may take a decade from the subtropics to the equatorial thermocline. To explicitly demonstrate this process, we regress the zonal mean temperature (170°E–150°W) on the STC index by different time lag. It can be seen in Figure 11 that warm signals are subducted in the midlatitude and then gradually penetrated to the low-latitude region and it takes about 10 years for them to reach the equator. Thus, this temperature anomaly changes the pressure gradient at low latitude, further to affect the STC eventually.

We argue in above analysis that the tropical cooling (warming) induced by accelerated (decelerated) STC can be advected to the midlatitude, therefore triggering a positive air-sea feedback. Detailed heat budget analysis is conducted to verify the above mentioned process. And the relevant mixed-layer heat budget equation is written as follows:

$$\frac{\partial T}{\partial t} = -\vec{V}_h \cdot \nabla T - W \frac{\partial T}{\partial z} + \frac{Q_{net}}{\rho C_p h} + R$$

where $\frac{\partial T}{\partial t}$ is temperature tendency, $-\vec{V}_h \cdot \nabla T$ is horizontal temperature advection, $-W \frac{\partial T}{\partial z}$ is vertical temperature advection, $\frac{Q_{net}}{\rho C_p h}$ is surface heat flux, and R denotes the residual term that includes the vertical entrainment, vertical and horizontal diffusions. Figure 12 shows the contributions of heat budget terms as the STC leads by 2 years. It is found that the midlatitude temperature anomaly is primarily associated with the horizontal advection (Figure 12a), while the surface heat flux plays a damping role (Figure 12b). Further decomposition in three key regions indicates that the influence of temperature advection by the mean meridional current $-\bar{V} \frac{\partial T'}{\partial y}$ is mainly concentrated at the western boundary region (Figures 13a and 13b), while the advection by the mean zonal current $-\bar{u} \frac{\partial T'}{\partial x}$ is in favor of transporting the heat from the western boundary to the central Pacific (Figures 13b and 13c). The advection by the anomalous meridional current $-V' \frac{\partial \bar{T}}{\partial y}$ also contributes positively (Figures 13a–13c). The physical interpretation can be summarized as follows: when the STC transport enhances, the equatorial SST becomes cooler as a result of cold water flux from higher latitudes. The opposite is true for the decreasing case. The anomalous tropical cooling is then transported to the midlatitude by the WBC and subsequently swept eastward by the North Pacific current.

5. Linkages Between PDO and STC in the South Pacific

The relationship between the PDO and Southern Hemispheric STC transport is shown in Figure 6b. Different from its counterpart in the Northern Hemisphere, the correlation between them is significant only when the

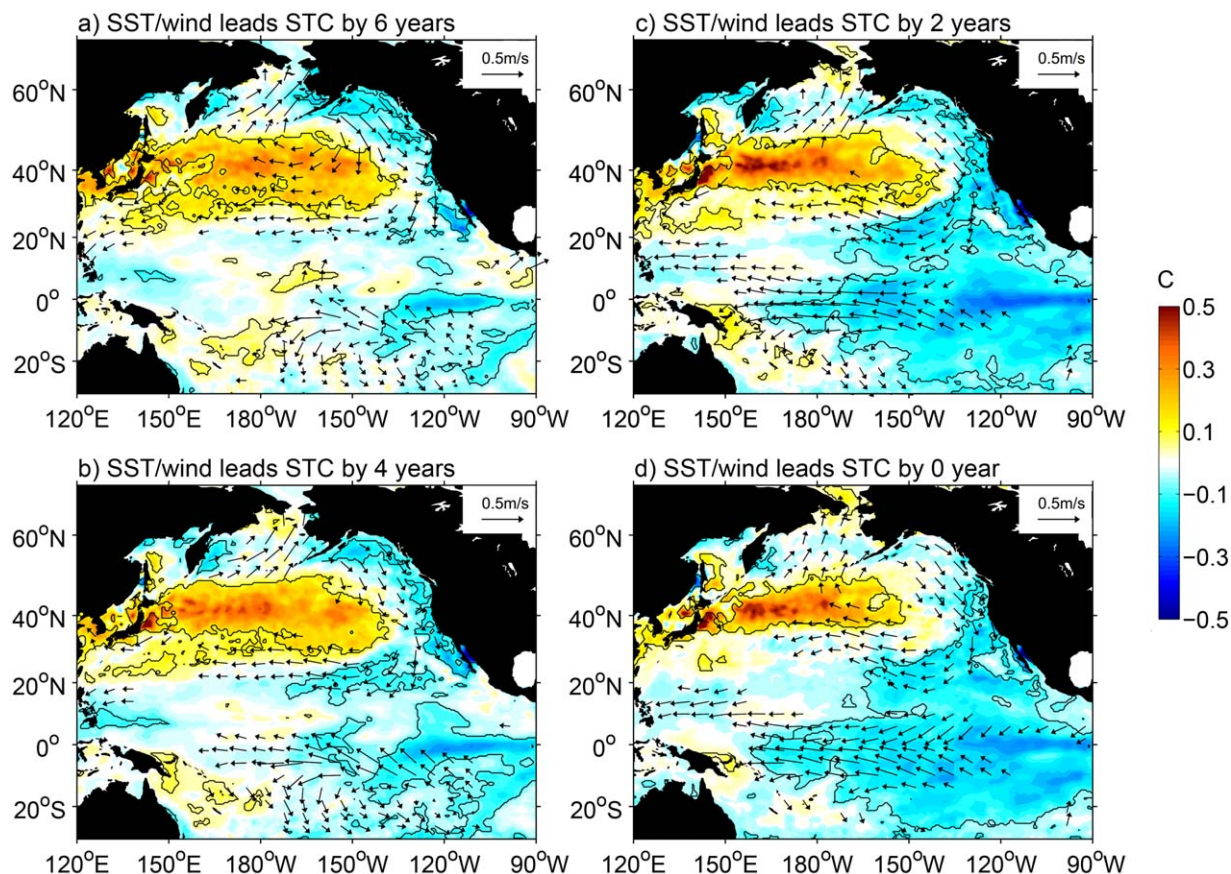


Figure 14. Same as Figure 7 but for 10°S . Shown are led regressions at (a) 6 years, (b) 4 years, (c) 2 years, and (d) 0 year.

PDO leads (Figure 6a versus Figure 6b). Further analysis reveals that the correlation reaches its minimum (-0.34) when the PDO leads the STC by 3 years while no significant correlation is detected as the STC leads the PDO. It implies that the Southern Hemispheric STC only responds passively to the PDO. We also conduct the regression analysis of the SST and surface wind on the STC index to clarify the linkages between the PDO and the STC transport at 10°S . As is displayed in Figure 14, the Pacific Ocean is occupied by a warming (cooling) pattern in the midlatitude and a cooling (warming) pattern in the east. Accordingly, the wind is characterized by an anticyclone (cyclone) in the midlatitude Pacific Ocean and strengthened (weakened) the northeast and southeast trade winds. Then the strengthened (weakened) southeast trade wind induces more (less) poleward Ekman transport in the surface and equatorward transport in the subsurface, which corresponds to a speed up (slowdown) of the STC.

6. Summary

The decadal variability of Pacific STC and its linkages with the PDO are investigated based on SODA 2.2.4. The analysis focuses on the decadal variability of pycnocline transports through the western boundary and interior across 10°N and 10°S . The decadal variations of boundary and interior pycnocline transports are found to be generally anticorrelated with each other, while the decadal variation of boundary pycnocline transport is less significant than that of the interior. This is different from the time-mean exchange where the boundary transport at 10°N is larger than the interior component. This indicates that the interior exchange in the Pacific Ocean is more important to decadal variability in the tropical Pacific.

It is found that an enhanced (reduced) STC strength corresponds to a strengthened (weakened) trade wind and a negative (positive) wind stress curl near 10°N (Figures 7e, 7f, 8e, and 8f), as proposed by Lee and

Fukumori [2003]. The trade wind affects the strength of the shallow meridional overturning circulation with a primarily equatorward (poleward) interior pycnocline flow and the latter changes the strength of the horizontal circulation and results in a variation of the boundary pycnocline flow. Similar mechanism works at 10°S as well.

The linkages between STC and PDO are investigated and it is found that the decadal variability of STC in the Northern Hemisphere is associated with the PDO. There is a negative (positive) correlation when the PDO leads (lags) the STC (10°N) transport. Here the PDO influence the STC transport mainly through two processes: changes in the northeast trades and density changes induced by subduction. The former is fast due to the first baroclinic mode adjustment, while the latter is related to second baroclinic mode adjustment at decadal time scales. Associated with a positive (negative) phase of PDO, the relaxation (acceleration) of the northeast trades slows down (spins up) the STC within a few years by baroclinic adjustment in conjunction with the subduction of the cold (warm) mixed-layer anomalies in the extratropics. The cold (warm) water is further injected into the thermocline and advected southwestward to the tropics along the isopycnal surfaces, leading to the slowdown (spin-up) of STC due to zonal pressure gradient change at low latitude. Along with the STC weakening (strengthening), a significant warming (cold) anomaly appears in the tropics and it is advected to the midlatitude by the Kuroshio and North Pacific currents, thus feeding back to the atmosphere over the North Pacific. Different from that in the Northern Hemisphere, the Southern Hemispheric STC primarily responds to the PDO passively. A negative (positive) phase of the PDO is associated with a strengthened (weakened) southeast trade wind, which leads to an increase (a decrease) of STC transport at 10°S.

The present study highlights the role of delayed wind and buoyancy forced adjustment of the STC to the PDO and horizontal gyre advection of the tropical SST anomalies to the midlatitudes in the decadal variability of the STC and PDO. This mechanism is different from the theory proposed by *Gu and Philander* [1997]. In their theory, the subduction process is suggested to play a delayed negative feedback to extratropical SST through returning tropical-to-extratropical atmospheric teleconnection. Here we suggest that the delayed adjustment of the STC can induce the changes in the tropical SST that can negatively feedback to the extratropical SST anomalies through horizontal gyre advection. This feedback may overwhelm the returning positive feedback of the tropical SST changes to the extratropics through atmospheric teleconnection.

It should be noted the present study is based on 138 years ocean reanalysis, which is somehow still short for studying the decadal variability. More analysis including the Coupled Model Intercomparison Project Phase 5 (CMIP5) is needed to further verify the linkages between PDO and STC on decadal time scales.

Acknowledgments

This research is supported by National Natural Science Foundation of China (NSFC) Key Project (41130859), China National Global Change Major Research Project (2013CB956201), NSFC Innovation Project (41221063), and the Research Project of Chinese Ministry of Education (113041A). Discussions with Bo Qiu, Michael McPhaden, and Shantong Sun are greatly appreciated.

References

- Bjerknes, J. (1964), Atlantic air-sea interaction, *Adv. Geophys.*, *10*, 1–82.
- Carton, J. A., and B. Giese (2008), A reanalysis of ocean climate using Simple Ocean Data Assimilation (SODA), *Mon. Weather Rev.*, *136*, 2999–3017.
- Chen, Z., and L. Wu (2011), Dynamics of the seasonal variation of the North Equatorial Current bifurcation, *J. Geophys. Res.*, *116*, C02018, doi:10.1029/2010JC006664.
- Compo, G. P., J. S. Whitaker, P. D. Sardeshmukh, N. Matsui, R. J. Allan, X. Yin, and S. J. Worley (2011), The twentieth century reanalysis project, *Q. J. R. Meteorol. Soc.*, *137*, 1–28.
- Frankignoul, C., and N. Sennéchal (2007), Observed influence of North Pacific SST anomalies on the atmospheric circulation, *J. Clim.*, *20*(3), 592–606.
- Gan, B., and L. Wu (2012), Modulation of atmospheric response to North Pacific SST anomalies under global warming: A statistical assessment, *J. Clim.*, *25*(19), 6554–6566.
- Giese, B. S., and S. Ray (2011), El Niño variability in Simple Ocean Data Assimilation (SODA), 1871–2008, *J. Geophys. Res.*, *116*, C02024, doi:10.1029/2010JC006695.
- Gu, D., and S. G. H. Philander (1997), Interdecadal climate fluctuations that depend on exchanges between the tropics and extratropics, *Nature*, *275*, 805–807.
- Huang, R. X. (2010), *Ocean Circulation: Wind-Driven and Thermohaline Processes*, 839 pp., Cambridge Univ. Press, Cambridge, U. K.
- Johnson, G. C., and M. J. McPhaden (1999), Interior pycnocline flow from the subtropical to the equatorial Pacific Ocean, *J. Phys. Oceanogr.*, *29*, 3073–3089.
- Kleeman, R., J. P. McCreary Jr., and B. A. Klinger (1999), A mechanism for generating ENSO decadal variability, *Geophys. Res. Lett.*, *26*, 1743–1746.
- Kushnir, Y., and I. M. Held (1996), Equilibrium atmospheric response to North Atlantic SST anomalies, *J. Clim.*, *9*(6), 1208–1220.
- Kushnir, Y., and N. C. Lau (1992), The general circulation model response to a North Pacific SST anomaly: Dependence on time scale and pattern polarity, *J. Clim.*, *5*(4), 271–283.

- Kushnir, Y., W. A. Robinson, I. Bladé, N. M. Hall, S. Peng, and R. Sutton (2002), Atmospheric GCM response to extratropical SST anomalies: Synthesis and evaluation, *J. Clim.*, *15*(16), 2233–2256.
- Latif, M., and T. P. Barnett (1994), Causes of decadal climate variability over the North Pacific and North America, *Science*, *266*, 634–637.
- Latif, M., and T. P. Barnett (1996), Decadal climate variability over the North Pacific and North America: Dynamics and predictability, *J. Clim.*, *9*(10), 2407–2423.
- Lee, T., and I. Fukumori (2003), Interannual-to-decadal variability of tropical-subtropical exchange in the Pacific Ocean: Boundary versus interior thermocline transports, *J. Clim.*, *16*, 4022–4042.
- Liu, Z. (1999), Planetary wave modes in the thermocline: Non-Doppler-shift mode, advective mode and Green mode, *Q. J. R. Meteorol. Soc.*, *125*, 1315–1339.
- Liu, Z., and L. Wu (2004), Atmospheric response to North Pacific SST: The role of ocean–atmosphere coupling, *J. Clim.*, *17*, 1859–1882.
- Lu, P., and J. P. McCreary Jr. (1995), Influence of the ITCZ on the flow of thermocline water from the subtropical to the equatorial Pacific Ocean, *J. Phys. Oceanogr.*, *25*, 3076–3088.
- Malanotte-Rizzoli, R., R. E. Young, K. Hedstrom, H. Arango, and D. B. Haidvogel (2000), Water mass pathways between the subtropical and tropical ocean in a climatological simulation of the North Atlantic ocean circulation, *Dyn. Atmos. Oceans*, *32*, 331–372.
- Mantua, N. J., S. R. Hare, Y. Zhang, J. M. Wallace, and R. C. Francis (1997), A Pacific interdecadal climate oscillation with impacts on salmon production, *Bull. Am. Meteorol. Soc.*, *78*, 1069–1079.
- McCreary, J. P., and P. Lu (1994), Interaction between the subtropical and equatorial ocean circulations: The subtropical cell, *J. Phys. Oceanogr.*, *24*, 466–497.
- McPhaden, M. J., and D. Zhang (2002), Slowdown of the meridional overturning circulation in the upper Pacific Ocean, *Nature*, *415*, 603–608.
- McPhaden, M. J., and D. Zhang (2004), Pacific Ocean circulation rebounds, *Geophys. Res. Lett.*, *31*, L18301, doi:10.1029/2004GL020727.
- Palmer, T. N., and S. Zhaobo (1985), A modelling and observational study of the relationship between sea surface temperature in the North-West Atlantic and the atmospheric general circulation, *Q. J. R. Meteorol. Soc.*, *111*(470), 947–975.
- Peng, S., A. Mysak, H. Ritchie, J. Derome, and B. Dugas (1995), The difference between early and middle winter atmospheric response to sea surface temperature anomalies in the northwest Atlantic, *J. Clim.*, *8*, 137–157.
- Peng, S., W. A. Robinson, and M. P. Hoerling (1997), The modeled atmospheric response to midlatitude SST anomalies and its dependence on background circulation states, *J. Clim.*, *10*, 971–987.
- Pitcher, E. J., M. L. Blackmon, G. T. Bates, and S. Muñoz (1988), The effect of North Pacific sea surface temperature anomalies on the January climate of a general circulation model, *J. Atmos. Sci.*, *45*(2), 173–188.
- Qu, T., and E. J. Lindstrom (2002), A climatological interpretation of the circulation in the Western South Pacific, *J. Phys. Oceanogr.*, *32*(9), 2492–2508.
- Schott, F. A., J. P. McCreary, and G. C. Johnson (2004), Shallow overturning circulations of the Tropical-Subtropical Oceans, in *Earth's Climate: The Ocean-Atmosphere Interaction*, *Geophys. Monogr. Ser.*, vol. 147, edited by C. Wang, S. P. Xie, and J. A. Carton, pp. 261–304, AGU, Washington, D. C.
- Schott, F. A., W. Wang, and D. Stammer (2007), Variability of the Pacific Subtropical Cells in the 50-year ECCO assimilation, *Geophys. Res. Lett.*, *34*, L05604, doi:10.1029/2006GL028478.
- Schott, F. A., L. Stramma, W. Wang, and B. Giese (2008), Pacific Subtropical Cell variability in the SODA 2.0.2/3 assimilation, *Geophys. Res. Lett.*, *35*, L10607, doi:10.1029/2008GL033757.
- Zhang, D., and M. J. McPhaden (2006), Decadal variability of the shallow Pacific meridional overturning circulation: Relation to tropical sea surface temperatures in observations and climate change models, *Ocean Modell.*, *15*, 250–273.
- Zhang, L., L. Wu, and L. Yu (2011a), Oceanic origin of recent La-Nina like warming trend in the Tropical Pacific, *Adv. Atmos. Sci.*, *28*, 1–9.
- Zhang, L., L. Wu, and J. Zhang (2011b), Coupled ocean-atmosphere responses to recent freshwater flux changes over the Kuroshio-Oyashio extension region, *J. Clim.*, *24*, 1507–1524.
- Zhang, L., L. Wu, and J. Zhang (2011c), Simulated response to recent freshwater flux change over the Gulf Stream and its extension: Coupled ocean–atmosphere adjustment and Atlantic–Pacific teleconnection, *J. Clim.*, *24*, 3971–3988.